Optical properties of thick GaInAs(Sb)N layers grown by liquid-phase epitaxy

You may also be interested in:

Investigation of the optical properties of InAs/InGaAs/GaAs quantum dot in quantum well multilayer structures for infrared photodetectors
Ts Ivanov, V Donchev, K Germanova et al.

Study of melt-grown GaAsN and InGaAsN epitaxial layers
P Vitanov, M Milanova, B Arnaudov et al.

Spectral photoconductivity and in-plane photovoltage of as-grown and annealed samples
A Erol, N Akcay, M C Arikan et al.

Investigation of Optical Absorption Spectra of GaAs/AlAs Multiple Quantum Wells Fabricated on a GaAs Substrate Using Surface Photovoltage and Piezoelectric Photothermal Techniques
Ping Wang, Shingo Kurayama, Atsuhiko Fukuyama et al.

Study of GaAsSb/GaAs type-II quantum well with top InAs quantum dot layer using complementary spectroscopy techniques
Hung-Pin Hsu, Jiun-De Wu, Yan-Jih Lin et al.

A vector model for analysing the surface photovoltage amplitude and phase spectra applied to complicated nanostructures
Ts Ivanov, V Donchev, K Germanova et al.

SPS characterization of InGaPN alloys
H P Hsu, P Y Wu, Y S Huang et al.

Optical properties of thick GaInAs(Sb)N layers grown by liquid-phase epitaxy

V Donchev[1,6], I Asenova[1,3], M Milanova[2], D Alonso-Álvarez[3], K Kirilov[1], N Shtinkov[4], I G Ivanov[5], S Georgiev[1], E Valcheva[1] and N Ekins-Daukes[3]

[1] Faculty of Physics, Sofia University, 5, J.Bourchier blvd., Sofia-1164, Bulgaria
[2] Central Laboratory of Applied Physics, 59 St. Petersburg blvd, 4000 Plovdiv, Bulgaria
[3] Department of Physics, Imperial College London, London, UK
[4] Department of Physics, University of Ottawa, Ottawa, ON, K1N 6N5, Canada
[5] Linköping University, Department of Physics, Chemistry & Biology, 581 83 Linköping, Sweden

E-mail: vtd@phys.uni-sofia.bg

Abstract. We present an experimental and theoretical study of GaInAs(Sb)N layers with thickness around 2 μm, grown by liquid-phase epitaxy (LPE) on n-type GaAs substrates. The samples are studied by surface photovoltage (SPV) spectroscopy and by photoluminescence spectroscopy. A theoretical model for the band structure of Sb-containing dilute nitrides is developed within the semi-empirical tight-binding approach in the $sp^3d^5s*s_N$ parameterisation and is used to calculate the electronic structure for different alloy compositions. The SPV spectra measured at room temperature clearly show a red shift of the absorption edge with respect to the absorption of the GaAs substrate. The shifts are in agreement with theoretical calculations results obtained for In, Sb and N concentrations corresponding to the experimentally determined ones. Photoluminescence measurements performed at 300K and 2 K show a smaller red shift of the emission energy with respect to GaAs as compared to the SPV results. The differences are explained by a tail of slow defect states below the conduction band edge, which are probed by SPV, but are less active in the PL experiment.

1. Introduction

Dilute nitrides form a novel class of semiconductor alloys, which has emerged from the conventional III-V compounds by doping with small amount of nitrogen. The addition of nitrogen in small concentrations has proven to have a significant influence on their electronic properties, in particular bandgap narrowing and shift of the absorption edge to longer wavelengths. This allows extended band structure engineering and makes the dilute nitrides materials of great interest for a variety of applications in advanced optoelectronic devices [1]. The addition of In in the alloy facilitates the

---

[6] To whom any correspondence should be addressed

incorporation of N, while Sb act as a surfactant that reduces the strain-induced defect formation, favours 2D growth and further decreases the bandgap [2].

While the conventional fabrication methods for dilute nitrides are molecular beam epitaxy (MBE) and metalorganic chemical vapour deposition (MOCVD), liquid phase epitaxy (LPE) has recently shown promise in obtaining high-quality dilute nitride layers with lower defect concentrations for optoelectronic applications [3,4]. This is related to the fact that LPE growth is carried out under near equilibrium conditions which provide high quality material in terms of lifetime, mobility and freedom from defects of the epitaxial layers. In spite of this the LPE technique has been rarely used for growing dilute nitrides alloys and the data on structural, optical and electronic properties of LPE-grown dilute nitride alloys are still scarce. Therefore, these materials need to be extensively studied.

Among the experimental techniques applied to dilute nitrides, surface photovoltage (SPV) spectroscopy has been relatively rarely used [5–7] although it provides information on the optical absorption spectrum and carrier transport in the sample [8]. Besides, the few reported SPV studies on dilute nitrides concern MBE or MOCVD grown samples. The present contribution partially fills this gap by presenting an original study of the electronic and optical properties of LPE-grown GaInAsN and GaInAsSbN layers based on SPV spectroscopy, combined with photoluminescence (PL) and semi-empirical tight-binding calculations.

2. Experimental

A series of $Ga_{1-y}In_yAs_{1-x}N_x$ and $Ga_{1-y}In_yAs_{1-x-z}Sb_zN_x$ epitaxial layers were grown by the horizontal graphite slide-boat technique for LPE on (100) n-type GaAs:Si (~10^{18}cm^{-3}) substrates. A flux of Pd-membrane purified hydrogen at atmospheric pressure was used for the experiments. No special baking of the system was carried out before epitaxy. The starting materials for the solutions consisted of 6N pure solvent metals Ga, In, Sb and of polycrystalline GaAs and GaN with purity of 5N. Quaternary $Ga_{1-y}In_yAs_{1-x}N_x$ layers with low In content were fabricated from mixed In+Ga melt, while for $Ga_{1-y}In_yAs_{1-x-z}Sb_zN_x$ layer growth a few percent of Sb were added to the melt. The N content in the melt was 0.5 at.% for all grown layers. Thick epitaxial layers were grown from initial epitaxy temperature varying in the range 590–550˚C at a cooling rate of 0.8˚C/min for 2–3 minutes. The layer thicknesses (1.5-2.5 µm) and compositions were determined using a scanning electron microscope LYRA I XMU (Tescan) equipped with an energy dispersive X-ray (EDX) microanalyzer (Quantax, Bruker). The In content in the layers varies in the range $0.02 \leq y \leq 0.03$ depending on the melt composition and epitaxy temperatures. Nitrogen content in the layers determined from HRXRD measurements using Vegard's rule is $0.002 \leq x \leq 0.003$.

SPV spectra were recorded at room temperature using the metal-insulator-semiconductor operation mode of the SPV technique [8]. The sample was illuminated by means of a 250 W halogen lamp along with a SPEX grating monochromator (f = 0.25 m, 600 gr/mm) and an optical chopper (94 Hz). The probe electrode was a semitransparent SnO_2 film evaporated on the bottom surface of a quartz glass separated from the sample by a sheet of mica (15 µm). The probe signal with respect to the ground was fed to a high-impedance unity gain buffer and then measured by an SR830 lock-in amplifier. The photon flux was kept constant ($\approx 1.5 \times 10^{14}$ cm^{-2}s^{-1}) within ± 0.5 % for all wavelengths, by positioning a neutral density filter with variable optical density. More details about the SPV experimental set-up and measurement procedure can be found in [9].

PL measurements at 300 K were performed using laser excitation at 532 nm (2.33 eV) with 4 mW (~50W/cm^2) power and at 405 nm (3.06 eV) with 50 mW (~4.5kW/cm^2). The signal was detected by a Si detector in the former case and by a CCD camera in the latter case. PL at 2K was also measured with 532 nm excitation. In this case a much lower excitation power (~100 mW/cm^2) was enough to obtain a strong PL signal, which was detected by a CCD camera.

The microscopic lattice structure related to the incorporation of N in InGaAsN alloys was studied by micro-Raman spectroscopy using Jobin Yvone LabRAM HR800 spectrometer and laser excitation at 632 nm.

3. Theoretical calculations

The electronic structure of $Ga_{1-y}In_yAs_{1-x}N_x$ and $Ga_{1-y}In_yAs_{1-x-z}Sb_zN_x$ was calculated using the semi-empirical tight-binding (TB) method for dilute nitrides in the $sp^3d^5s^*s_N$ parameterization, including the spin-orbit coupling [10]. The effects of the addition of nitrogen on the band structure were considered independent from those of In and Sb [11], allowing us to use the virtual crystal approximation for the TB parameters of the GaInAsSb quaternary. Quadratic corrections were introduced to account for the large GaAsSb band gap bowing parameter of 1,43 eV [12]. The N-related TB parameters previously derived for the $Ga_{1-y}In_yAs_{1-x}N_x$ and $GaP_{1-x}N_x$ dilute nitride alloys were used [11], with valence band offsets with respect to GaAs of 0.21 eV, 0.77 eV, and 0.80 eV for the unstrained InAs, GaSb, and InSb, respectively [12]. The bandgap reduction with respect to pure GaAs was calculated for N, In, and Sb concentrations in the expected experimental range ($x \leq 0.01$; $y \leq 0.10$; $z \leq 0.02$).

4. Results and discussions

In figure 1a the SPV amplitude spectrum of a $Ga_{1-y}In_yAs_{1-x}N_x$ sample is compared with its PL spectrum and the SPV spectrum of the GaAs substrate. The small undulations in the SPV spectrum are due to the interference effects caused by the mica sheet. A clear red shift of the absorption edge with respect to GaAs is evidenced by the comparison of the SPV spectra. To assess the bandgap of the material we plot the square of the SPV vs photon energy, which for the ideal case of a bulk semiconductor should give a straight line resulting from the shape of the 3D combined density of states. In the present case we consider the linear part of the obtained curve and extrapolate the straight line to find its intersection with the abscissa, which is assumed to be the bandgap, E_g. For the current sample $E_g = 1.328$ eV and therefore the bandgap shift ΔE_g with respect to GaAs (E_g=1.423 eV) is 95 meV. The same result (within the experimental error) is obtained by using Tauc plot assuming that SPV is proportional to the absorption coefficient. On the other hand the PL peak position is at 1.362 eV, i.e. 34 meV higher that the bandgap determined from the SPV results.

In figure 1b the SPV amplitude spectrum of a $Ga_{1-y}In_yAs_{1-x-z}Sb_zN_x$ sample is compared with its PL spectrum and the SPV spectrum of the GaAs substrate. The bandgap determined from the SPV curve is 1.312 eV. Therefore the bandgap shift ΔE_g with respect to GaAs is 111 meV in this case. The PL peak appears at 1.357 eV, i.e. 45 meV higher than the bandgap determined from the SPV results.
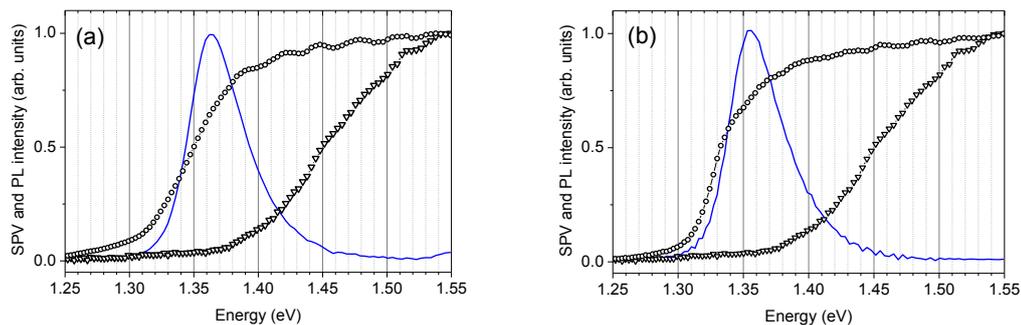

Figure 1. SPV (circles) and PL (line) spectra of a $Ga_{1-y}In_yAs_{1-x}N_x$ (a) and a $Ga_{1-y}In_yAs_{1-x-z}Sb_zN_x$ (b) sample measured at room temperature. The SPV spectra of the GaAs substrate are represented by triangles.

The above described comparisons between SPV and PL were performed for a number of $Ga_{1-y}In_yAs_{1-x}N_x$ and $Ga_{1-y}In_yAs_{1-x-z}Sb_zN_x$ samples. The results show a clear decrease of the bandgap of the dilute alloy with respect that of GaAs. The addition of Sb further reduces the bandgap, which is in accordance with literature data [2]. On the other hand there is a clear discrepancy between the bandgap energy determined from SPV and the position of the PL peak – the values found by SPV are lower

than that from PL by some 30-45 meV depending on the sample. This is a kind of "anti-Stokes shift" and is opposite to the Stokes shift between SPV and PL reported in [6] for $Ga_{1-y}In_yAs_{1-x}N_x$ samples with $y = 0.72$ and x ranging from 0.009 to 0.017.

A few $Ga_{1-y}In_yAs_{1-x}N_x$ samples were measured by PL at 2K. A typical 2K PL spectrum is represented by solid line in figure 2, together with the room temperature SPV (circles) and PL (dashed line) spectra. For the purposes of comparison the origin of the energy axis is set at the GaAs bandgap at the corresponding temperature, namely 1.519 eV for 2K and 1.423 eV for 300 K. This way we compare the shifts with respect to the GaAs bandgap rather than the bandgaps themselves. The 2K PL spectrum reveals a peak at –51 meV and a tail from its low-energy side with many small peaks on it. The PL peak obtained at 300 K is much broader but is located at the same energy position as the 2K PL peak. Therefore the PL peaks at 2K and 300 K show the same bandgap red shift of 51 meV with respect to the GaAs bandgap at the corresponding temperature. The SPV spectrum reveals the usual step. Applying the procedure described above gives a bandgap shift with respect to GaAs of 83 meV. Thus, again a discrepancy between SPV and PL results is observed (32 meV in the present case) indicating higher bandgap transition energies for PL.
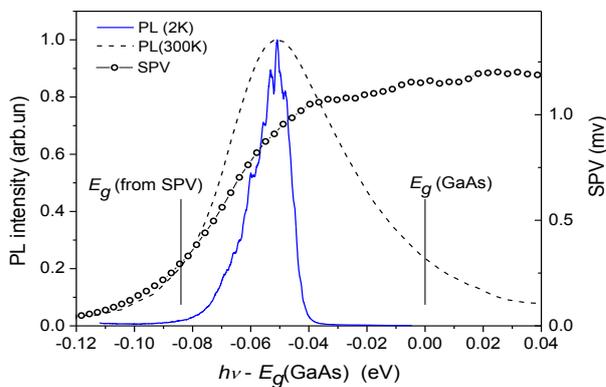

Figure 2. PL of a $Ga_{1-y}In_yAs_{1-x}N_x$ sample measured at 300 K (dashed line) and 2 K (solid line) compared to its 300 K SPV spectrum (circles). The energy is measured from the GaAs bandgap at the corresponding temperature.
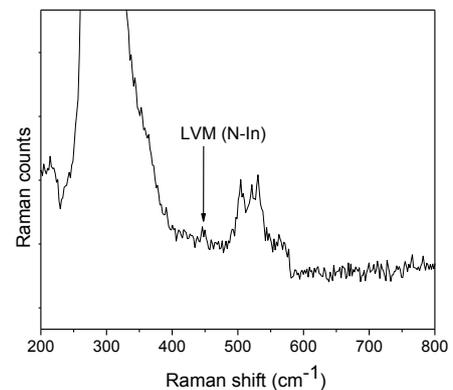
Figure 3. Raman spectrum of as grown InGaAsN layer showing local vibration modes of N-In.

A tentative explanation of these discrepancies is presented below. In an ideal case all N atoms introduced in the crystal take places of As atoms. In figure 3 by means of micro-Raman spectroscopy N-induced local mode is observed in the range 440 to 460 cm^{-1} providing evidence for the formation of In-N bonds. In practice the N atoms take various positions in the crystal lattice as well as form clusters. This results in a series of defect states, some of which are in the bandgap. We assume that these states are slower with respect to recombination (e.g because the electron has to overcome an energy barrier before recombination) than the extended states in the conduction band. The light intensity in the SPV experiment is much lower than that in the PL one. So, with increasing photon energy, SPV probes first these states and as a result gives a relatively low optical transitions energy. On the other hand under laser excitation, which is the case of the PL experiment, these states are filled with electrons. As they are less effective for radiative recombination, the PL mainly probes states with higher energies, which are faster and more effective for emission. Thus, the PL peak appears at higher energies than the bandgap obtained by SPV. The existence of a tail of defect states in the bandgap is evidenced by the low-energy tail of the 2K PL spectrum. If there is an activation barrier for radiative recombination via the slow centres, the low temperature makes further difficult the overcoming of this

barrier. Similar PL results were obtained in [13] for $GaAs_{1-x}N_x$ ($x \sim 0.25\%$) and explained by localized and delocalized defect states below the GaAs conduction band. A continuous distribution of shallow defect states located just below the conduction band edge of $Ga_{1-y}In_yAs_{1-x}N_x$ is reported in [14].
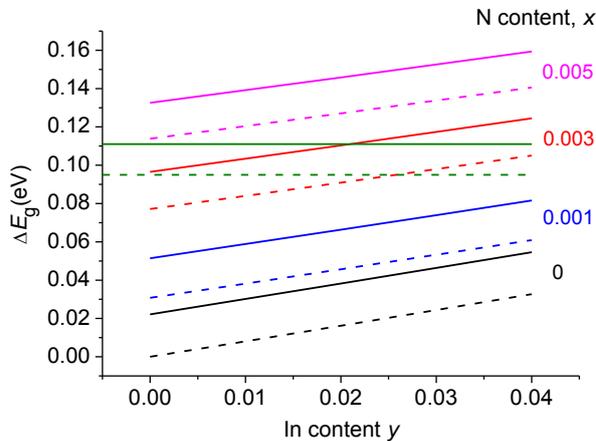
Figure 4. Calculated bandgap shifts of $Ga_{1-y}In_yAs_{1-x-z}Sb_zN_x$ as a function of the In content, for Sb concentrations of 1% (solid lines) and 0% (dotted lines). Curves of different colours correspond to different N fractions as shown. The horizontal lines indicate the experimental shifts obtained by SPV for the samples from figure 1.

Figure 4 shows the calculated dependences of the bandgap shift with respect to GaAs in the expected range of N, In, and Sb concentrations. The addition of Sb reduces the bandgap with 22 meV/at. %, which is in agreement with recent experimental results showing a value of $\approx$20 meV/at. % for both pure ternary [15] and dilute nitride [16]. This demonstrates the validity of the $sp^3d^5s^*s_N$ model for calculating the bandgap energies of dilute nitrides containing Sb, and validates the use of universal N-related TB parameters for all dilute III-V nitrides. Remarkably, the behaviour of the pentanary $Ga_{1-y}In_yAs_{1-x-z}Sb_zN_x$ is described without introducing new parameters to the standard $sp^3d^5s^*s_N$ parameterization [10,11]. Figure 4 also shows that the calculated bandgap shifts corresponding to the experimentally found In content of 0.02–0.03 and N content of around 0.003 are 91–97 meV for the case without Sb and 110–117 meV for the case of 1% Sb. These values are in good agreement with the experimental values of 95 meV and 111 meV, respectively determined by SPV.

5. Conclusion
An original study of the optical properties of thick LPE grown GaInAs(Sb)N layers is presented. The absorption features, measured by SPV spectroscopy, are compared with results obtained by PL and tight-binding calculations in terms of bandgap shift with respect to GaAs. The bandgap shifts found by SPV are of the order of 80–95 meV for the samples without Sb and around 100–110 meV for the samples containing Sb. They are in good agreement with the calculation results, while the bandgap shifts determined by PL are 30–45 meV lower. This is explained by the existence of a tail of slow defect states just below the conduction band edge, which are probed by SPV, but are less active in the PL experiment. This work demonstrates the ability of the SPV technique as an alternative of the optical absorption spectroscopy for studying dilute nitride materials. The obtained results contribute to better understanding of the physical properties of dilute nitrides grown by LPE and their potential for optoelectronic applications.

References
[1] Erol E A, ed. 2008 *Dilute III-V Nitride Semiconductors and Material Systems. Physics and Technology* (Berlin: Springer)

[2]   Fehse R and Adams A R 2004 Recombination Processes in GaInNAs Long-Wavelength Lasers, in: *Physics and Applications of Dilute Nitrides*, ed I.A. Buyanova and W. Chen (New York, Taylor & Francis) pp. 362–394

[3]   Dhar S, Halder N, Kumar J and Arora B M 2004 Observation of a 0.7 eV electron trap in dilute GaAsN layers grown by liquid-phase epitaxy *Appl. Phys. Lett*. **85** 964–66

[4]   Milanova M, Vitanov P, Terziyska P, Popov G and Koleva G 2012 Structural and electrical characteristics of InGaAsN layers grown by LPE *J.Crystal Growth* **346** 79-82

[5]   Kudrawiec R et al. 2014 Surface photovoltage and modulation spectroscopy of E_- and E_+ transitions in GaNAs layers *Thin Solid Films* **567** 101–104

[6]   Bansal B, Kadir A, Bhattacharya A, Arora B M and Bhat R B 2006 Alloy disorder effects on the room temperature optical properties of GaInNAs quantum wells *Appl. Phys. Lett.* **89** 032110

[7]   Donchev V, Milanova M, Lemieux J, Shtinkov N and Ivanov I G 2016 Surface photovoltage and photoluminescence study of thick Ga(In)AsN layers grown by liquid-phase epitaxy *J. Phys. Conf. Ser.* **700** 012028

[8]   Kronik L and Shapira Y 1999 Surface photovoltage phenomena: Theory, experiment, and applications *Surf. Sci. Rep.* **37** 1–206

[9]   Donchev V, Ivanov T, Germanova K and Kirilov K 2010 Surface photovoltage spectroscopy – an advanced method for characterization of semiconductor nanostructures *Trends in Applied Spectroscopy* **8** 27–66

[10]   Shtinkov N, Desjardins P and Masut R 2003 Empirical tight-binding model for the electronic structure of dilute GaNAs alloys *Phys. Rev.* B. **67** 081202

[11]   Turcotte S, Shtinkov N, Desjardins P, Masut R and Leonelli R 2004 Empirical tight-binding calculations of the electronic structure of dilute III–V–N semiconductor alloys *J. Vac. Sci. Technol.* A **22** 776

[12]   Vurgaftman I, Meyer J R and Ram-Mohan L R 2001 Band parameters for III–V compound semiconductors and their alloys *J. Appl. Phys*. **89** 5815

[13]   Bhuyan S, Das S K, Dhar S, Pal B and Bansal B 2014 Optical density of states in ultradilute GaAsN alloy: Coexistence of free excitons and impurity band of localized and delocalized states *J. Appl. Phys*. **116** 023103

[14]   Kaplar R J, Ringel S A, Kurtz S R, Klem J F and Allerman A A 2002 Deep-level defects in InGaAsN grown by molecular-beam epitaxy *Appl. Phys. Lett*. **80** 4777–4779

[15]   Bian L F, Jiang D S, Tan P H, Lu S L, Sun B Q, Li L H , et al. 2004 Photoluminescence characteristics of GaAsSbN/GaAs epilayers lattice-matched to GaAs substrates *Solid State Commun.* **132** 707–711

[16]   Wang T S, Tsai J T, Lin K I, Hwang J S, Lin H H and Chou L C 2008 Characterization of band gap in GaAsSb/GaAs heterojunction and band alignment in GaAsSb/GaAs multiple quantum wells *Mater. Sci. Eng. B* **147** 131–135